JACS
JOURNAL OF THE AMERICAN CHEMICAL SOCIETY
Article
pubs.acs.org/JACS

Toward a Chemical Marker for Inflammatory Disease: A Fluorescent Probe for Membrane-Localized Thioredoxin

Min Hee Lee,[†,§] Hyun Mi Jeon,[‡] Ji Hye Han,[‡] Nayoung Park,[§] Chulhun Kang,*[,‡] Jonathan L. Sessler,*[,†] and Jong Seung Kim*[,§]

[†]Department of Chemistry, The University of Texas at Austin, Austin, Texas 78712-1224, United States
[‡]The School of East-West Medical Science, Kyung Hee University, Yongin 446-701, Korea
[§]Department of Chemistry, Korea University, Seoul 136-701, Korea

Supporting Information

ABSTRACT: Thioredoxin (Trx) is a redox-active protein that plays a key role in mitigating the effects of oxidative stress. The secretion of Trx on the plasma membrane has been suggested as a distinctive feature of inflammation. However, selective monitoring of membrane-associated Trx activity has proved challenging because of the ubiquity of Trx action in cells. Here, we report a Trx-specific probe that allows visualization of Trx activity associated with the membranes via fluorescence microscopy. The ability of this probe to act as a possible screening tool for agents that modulate Trx secretion was demonstrated in HeLa cells under oxidative stress conditions and in a cellular hepatosteatosis model. Control experiments serve to confirm that the response seen for the present probe is due to Trx and that it is selective over various potentially competing metabolites, including thiol-containing small molecules and test proteins.

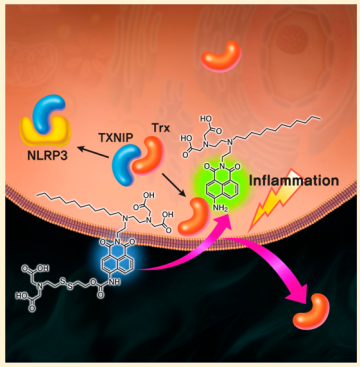

INTRODUCTION

Thioredoxin (Trx), along with Trx reductase and NADPH, comprises an important component of the cellular antioxidant system. Trx contains two adjacent Cys residues in its active site, and their oxidation to the corresponding disulfide serves to transfer reducing equivalents (re)supplied by Trx reductase and NADPH. The Trx redox system plays a number of critical roles in cells,[1] including reduction of oxidized proteins,[2] scavenging reactive oxygen species (ROS),[3] regulating cell signaling,[4] controlling growth,[5] and mediating both anti-apoptotic[6] and anti-inflammation[7] functions. Its biological importance is underscored by the fact that non-homeostatic Trx levels are seen in several types of cancers,[8] cardiovascular disease,[9] and diabetes,[10] as well as in inflammation.[11]

Although Trx is relatively ubiquitous in cells, its expression at specific locations may be implicated in different diseases. For instance, increased Trx within the nucleus or in the cytosol has been observed in the case of many cancers.[12] In contrast, it has been suggested that membrane-associated Trx may be an indicator of inflammation.[3,7,13−17] Having tests for Trx that are specific to different subcellular locales could be useful in discriminating between different Trx-releasing determinants and thus differentiating between various disease states. This could allow for improved diagnoses and obviate the need for invasive procedures, such as tissue biopsies.

In the case of inflammation, Trx on the plasma membrane is secreted to the extracellular medium in response to oxidative stress, and the released Trx engenders cytoprotective effects under oxidative stress and inflammatory conditions.[3,7,13−17] Membrane-localized Trx activity might thus be a good clinical marker for the anti-inflammatory action of cells. So far, it has been shown that most human cell lines have a membrane-associated Trx, as inferred from indirect immunofluorescence and Western blotting analyses.[14−16] However, the activity of membrane-localized Trx and the mechanism of its secretion in association with an inflammatory insult are not fully understood. Since the oxidation of Trx on the membrane triggers a cellular inflammatory response, a readily available fluorescent probe that would allow Trx activity to be monitored directly at (or around) membrane sites is expected to be particularly useful. The probe could cast new light on the mechanism of Trx action during inflammation and allow the study of inflammation-related disease via optical methods. Ultimately, such a locus-specific Trx sensor system could allow for diagnoses to be made without the need for invasive procedures.

Currently, we are unaware of any fluorescence probe that may be used for the determination of membrane-associated Trx activity. Trx probes are, however, known. For instance, we previously reported a fluorescent probe that can visualize mitochondrial Trx activity (as opposed to membrane-localized Trx activity) in living cells.[18] This system proved highly specific for Trx. Thus, building off this prior work, we have developed a new membrane-targeted Trx-specific fluorescent probe. As detailed below, this new system, probe **1**, acts as a chemical marker for inflammation.

Received: April 3, 2014
Published: May 19, 2014

dx.doi.org/10.1021/ja503356q | J. Am. Chem. Soc. 2014, 136, 8430−8437

Scheme 1. Schematic Representation of the Reaction of 1 with the Membrane-Localized Trx[a]

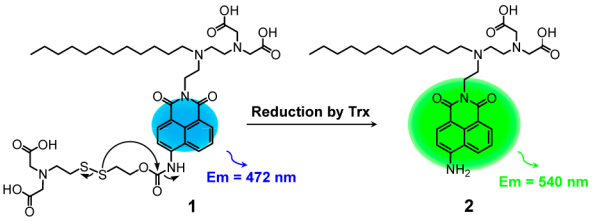

[a]As detailed in the present report, probe **1** interacts with the lipid bilayer of a cell membrane, where Trx-induced reduction of the disulfide bond triggers a fluorescence change.

RESULTS AND DISCUSSION

We report a fluorescent sensor (probe **1**) that allows for the selective visualization of membrane-associated Trx activity in a cell-based inflammation model. As can be seen from an inspection of its chemical structure (Schemes 1 and 2), probe **1** is composed of a disulfide-linked naphthalimide, a dodecyl alkyl chain, and four carboxylic acid groups. The lipophilic alkyl chain serves to guide the probe **1** to the cell membrane, while the four hydrophilic carboxylic acid groups delay its subsequent diffusion across the membrane. The disulfide-linked naphthalimide moiety[18] is preferentially reduced by Trx with an approximately 5000-fold faster reaction rate than that mediated by GSH; this disulfide reduction and corresponding bond cleavage provides an easy-to-monitor fluorescent signal at 540 nm, as illustrated in Scheme 1.

Probe **1** was prepared by the synthetic route outlined in Scheme 2. Two references, compounds **2** and **12**,[18] without a disulfide linkage and without the dodecyl alkyl chain and four carboxylic acid groups, respectively, were also prepared for the comparison (Scheme 2). Their chemical structures were confirmed by ^{1}H and ^{13}C NMR spectroscopy, MALDI-TOF mass spectrometry (MS), and ESI-MS (Figures S18−S47). The synthesis of compounds **1**−**12** is described fully in the Supporting Information.

The UV/vis absorption and fluorescence features of **1** were studied in the presence of metabolic thiols, essential metal ions, and hydrogen peroxide (H_2O_2) at 37 °C in phosphate-buffered saline (PBS) at pH 7.4. Addition of **1** to PBS solutions containing biological thiols, such as Trx, glutathione (GSH), homocysteine (Hcy), and cysteine (Cys), led to a shift in the absorption and emission bands of the probe from 376 and 495

Scheme 2. (a−c) Synthetic Routes to Compounds 5, 10, 1, and 2 and (d) Structure of the Reference Compound 12[a]

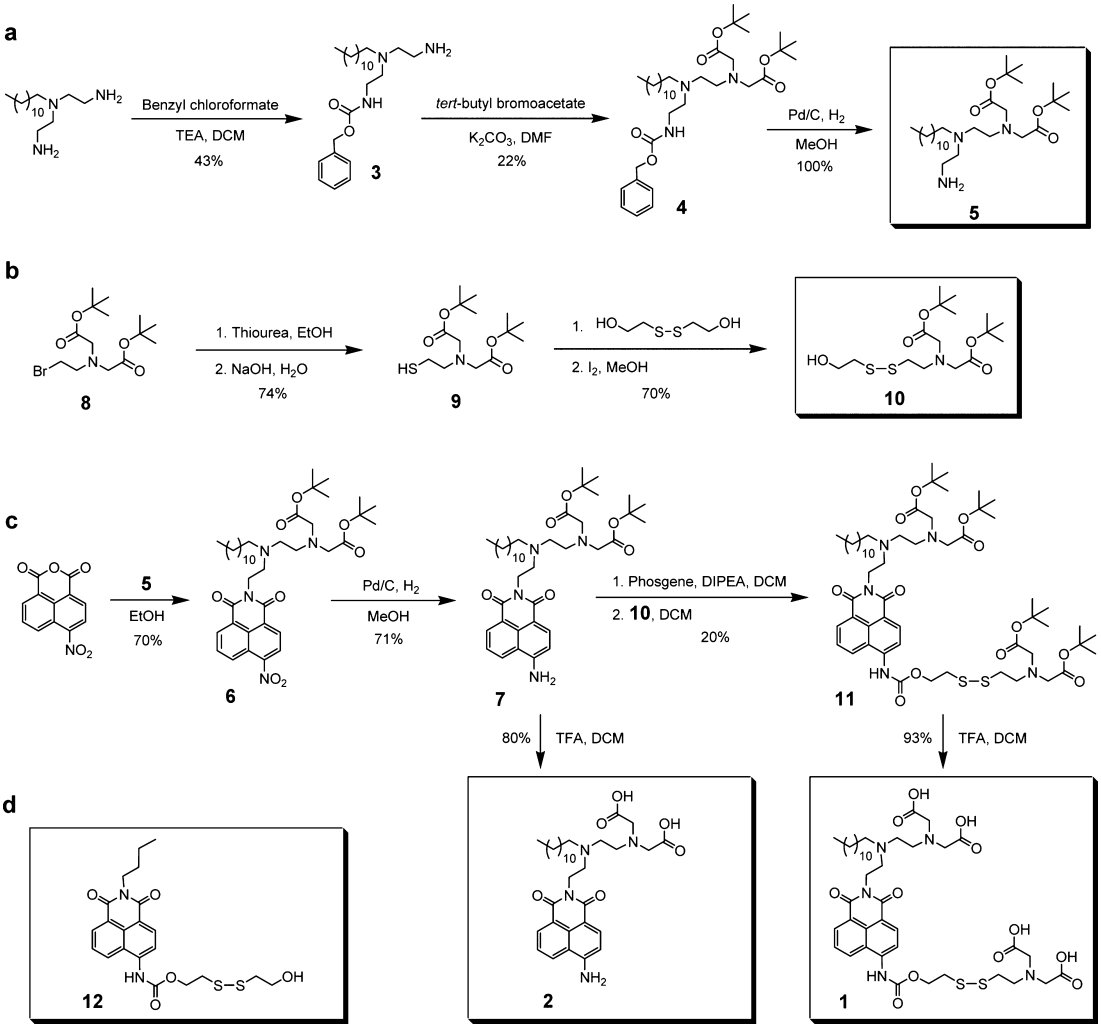

[a]TEA, triethylamine; DCM, dichloromethane; DMF, *N,N*-dimethylformamide; DIPEA, *N,N*-diisopropylethylamine; TFA, trifluoroacetic acid.

dx.doi.org/10.1021/ja503356q | J. Am. Chem. Soc. 2014, 136, 8430−8437

to 430 and 540 nm, respectively (Figure S1). In contrast, no such significant changes were observed upon exposure to other putative analytes. Of note is that, in the presence of 5.0 μM Trx, the fluorescence intensity (FI) of **1** at 540 nm was enhanced by ca. 9-fold. This is a greater enhancement than seen in the presence of 5 mM of other test biological thiols, viz. GSH, Cys, and Hcy. Typical intracellular Trx levels (ca. 5−10 μM) are roughly 1000-fold lower than those of other biological thiols.[18,19] Thus, the selectivity displayed by **1** was thought to augur well for its use as a membrane-localized, Trx-specific probe. Evidence in support of this postulate is provided below.

As a first step toward confirming the sensitivity, the fluorescence spectra of **1** were recorded at various Trx concentrations (0−5.0 μM). The induced changes were found to reach a plateau upon the addition of 1.0 equiv of the probe, and over this 0−1 equiv regime, a linear relationship (R^2 = 0.9853) between the FI at 540 nm and the Trx concentration was observed (see Figure 1a,b). Based on a

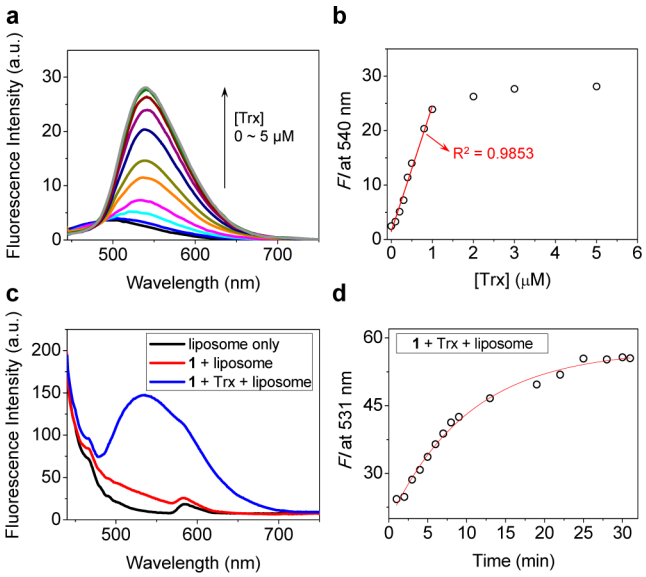

Figure 1. Trx-induced changes in the photophysical properties of probe **1** in PBS solution and liposomes. (a) Fluorescence changes of **1** (1.0 μM) observed upon treatment with increasing concentrations of Trx (0−5.0 μM). (b) Change in the fluorescence intensity (FI) at 540 nm as a function of Trx concentration. Spectra in panels (a) and (b) were acquired 30 min after addition of Trx and were recorded in PBS solution (pH 7.4) containing 5% (v/v) of DMSO at 37 °C. (c) Fluorescence spectra of **1** (5.0 μM) recorded in the absence (red line) and presence (blue line) of Trx (5.0 μM). Black line represents liposome (DPPC/40 mol% cholesterol) only. Data were acquired 30 min after mixing **1** with Trx in the liposome at 37 °C. (d) Time course of the fluorescence response of **1** (1.0 μM) with Trx (5.0 μM) in liposomes. Excitation was effected at 430 nm.

MALDI-TOF mass spectrometric analysis of the reaction product, we suggest that under these conditions probe **1** is converted to $[\mathbf{2}+H]^+$ (Figure S2). In addition, the absorption and fluorescence spectra of the product produced when **1** is exposed to Trx are fully consistent with those of **2** as prepared through independent synthesis (Figure S3). On this basis, we suggest that probe **1** has the sensitivity needed to be used as a membrane-localized Trx sensor.

To test the above assumption in a hydrophobic environment designed to model that of the cell membrane, probe **1** was embedded into a liposome composed of 1,2-dipalmitoyl-*sn*-glycero-3-phosphocholine (DPPC) and 40 mol% cholesterol (cf. Figure 1c,d). The liposomes were prepared in accord with literature procedures[20] and characterized by transmission electron microscopy (TEM) (Figure S4). In accord with design expectations, Trx in solution was found to react with **1** embedded in the liposome and produce a large fluorescence enhancement at 531 nm (Figure 1c); presumably, this enhancement reflects disulfide bond cleavage in accord with the scenario presented in Scheme 1. The maximum emission wavelength in liposomes is slightly blue-shifted compared with that in PBS solution. A linear relationship (R^2 = 0.9826) between the FI at 531 nm and the Trx concentration (0−1.0 equiv) was found (Figure S5). The fluorescence changes of **1** (1.0 μM) in the liposomal formulation were also monitored as a function of time in the presence of 5.0 μM Trx. It was found that the FI at 531 nm increases gradually and reaches a plateau within 30 min (Figure 1d).

To provide support for the notion that **1** can be used to detect cellular Trx pools with negligible interference from other biologically relevant analytes in membrane-like environments, the fluorescence change seen for **1** in the presence of other potential interferants, including GSH, Cys, Hcy, H_2O_2, and several test biologically relevant metal ions, was recorded in liposomes. We found the spectral changes are similar to the results shown in Figure 1, except that extent of cleavage (of probe **1**) and associated optical changes produced by GSH decrease is reduced in liposomes. Trx-based activity remains high (cf. Figure S6).

Using confocal microscopy, the fluorescence changes of HeLa cells treated with **1** were monitored as a function of time (1−60 min) (Figure S7). This was done in order to obtain insights into the cellular loci where probe **1** undergoes thiol-mediated disulfide cleavage. Results from these experiments are presented in Figure 2a, which shows confocal microscopy images obtained at 1, 5, and 20 min after incubation with the probe. These images are displayed as green, red, and blue-colored images, respectively, and are overlaid to give various pseudo color images (1 + 5 min, 5 + 20 min, and 1 + 5 + 20 min, respectively). An intense fluorescence signature resulting from the disulfide cleavage of **1** begins to appear around the cell membrane by 1 min (see green color in the overlay image of 1 + 5 + 20 min). This intensity subsequently diffuses into the cytosol where it is apparent by minute 20.

In contrast to what is true for probe **1**, compound **2**, the fluorescent product of the cleavage reaction of **1**, shows a fast cellular uptake into the cytosol of the cells without the membrane associated fluorescence features seen in the case of **1** (Figure S8). On the basis of these observations, we suggest that in the case of **1** disulfide bond cleavage occurs near the cell membrane to generate a daughter product (fluorescent species **2**), which then diffuses into the cytosol. In the case of **12**, a reference compound lacking a dodecyl alkyl chain and the four carboxylic acid groups found in **1**, similar experiments reveal a near complete absence of membrane-associated FI (Figure S9).

To provide further support for the suggestion that a membrane-associated fluorogenic disulfide bond cleavage reaction involving **1** is followed by the endocytotic transfer of the resulting fluorescent product (**2**) into the interior of the cells, experiments analogous to the above were performed in the presence of methyl-β-cyclodextrin (MCD). MCD is a known inhibitor of caveolae-dependent endocytosis and its effect is concentration dependent.[21] It can thus be used to test whether lipophilic compounds are being internalized into cells

dx.doi.org/10.1021/ja503356q | J. Am. Chem. Soc. 2014, 136, 8430−8437

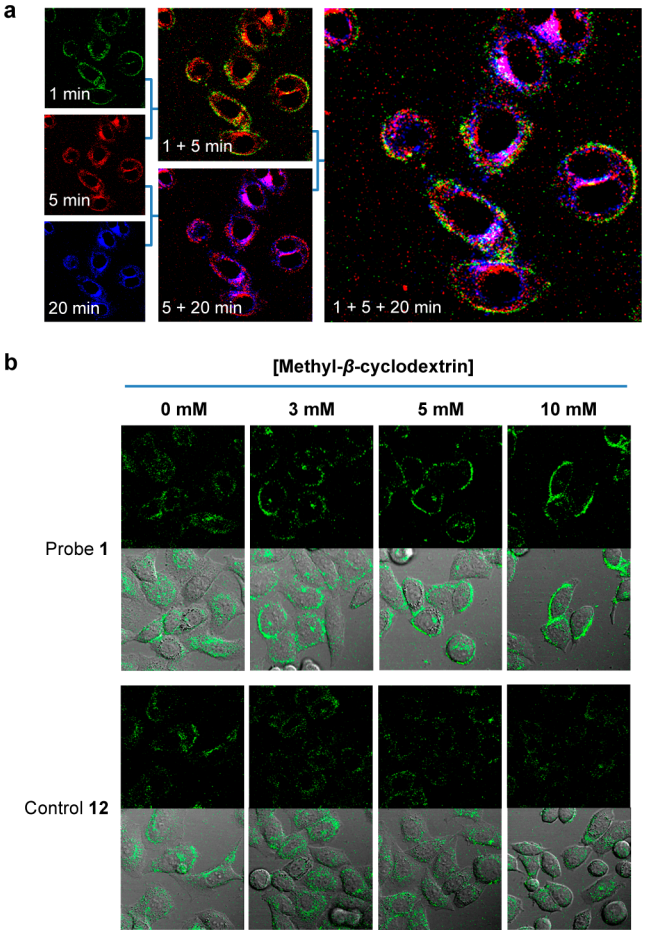

Figure 2. Confocal microscopy images of HeLa cells showing the fluorogenic response as a function of time after incubation with probe **1** and the effect of methyl-β-cyclodextrin (MCD) on the cell environment-induced changes in the fluorescence features of probes **1** and **12**. (a) HeLa cells were incubated with PBS containing **1** (5.0 μM) at 37 °C. The images were obtained at time points consisting of 1, 5, and 20 min after the addition of **1**. The intensities of the images were then adjusted to be similar to allow for direct comparisons. Finally, the images were merged, 1 + 5 min, 5 + 20 min, and 1 + 5 + 20 min. (b) Confocal microscopy images and overlay with the corresponding differential interference contrast images of HeLa cells treated with **1** and **12**, respectively. The studies were carried out in the absence and presence of MCD. Here, the cells were separately pretreated with media containing MCD (0, 3, 5, and 10 mM) and incubated for 1 h at 37 °C. The media were replaced with PBS containing **1** (5.0 μM) or **12** (1.0 μM). After 5 min, the fluorescence images were recorded.

via the caveolae pathway.[22] In accord with our hypothesis, probe **1** was found to undergo a fluorogenic reaction regardless of the presence or absence of MCD. On the other hand, the fluorescent signal ascribed to daughter product **2** is observed near the membrane in a MCD dose-dependent manner (cf. upper panels in Figure 2b). Finally, the fluorogenic response produced by control **12** was seen to decrease gradually as the concentration of MCD increased (lower panels in Figure 2b); this is expected for a system where disulfide cleavage takes place predominantly within the cytosol. The contrasting behavior between **1** and **12** is fully consistent with the proposition that probe **1** targets the membrane-associated thiols to give a fluorescence change as depicted in Scheme 1.

To confirm the site of initial fluorogenic reaction of probe **1**, colocalization experiments were carried out using a fluorescent membrane tracker (DiIC12) and with an early endosome tracker (Early Endosomes-RFP). As shown in Figure S10, the fluorescence image of **1** partially overlaps with those produced by the membrane tracker, and mostly at the cytosolic side of the membrane (panels a–d in Figure S10). On the other hand, a poor fluorescence overlap was seen in the colocalization studies involving the early endosome tracker (panels e–h in Figure S10). From these experiments, we infer that the thiol-induced fluorogenic reaction of **1** (1) is membrane associated, (2) involves predominantly thiols that are present on the cytosolic side of the membrane and (3) is not dependent on an endocytotic process.

To identify the thiol species responsible for the fluorogenic reaction of **1** shown in Figure 2, the cells were treated with PX-12, a selective Trx inhibitor.[18,23] As can be seen from an inspection of the upper panels of Figure 3, the FI of the HeLa

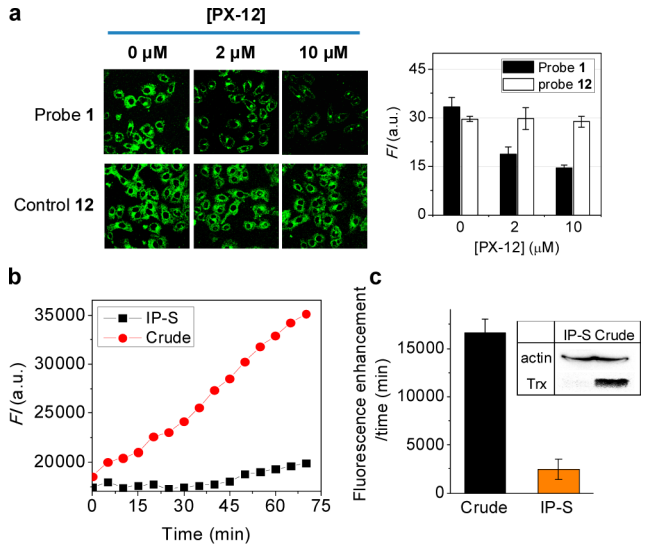

Figure 3. Changes in the fluorescence emission features of **1** and a control system (**12**) seen in HeLa cells and in protein extract. (a) Effect of PX-12, a selective inhibitor of Trx, on the fluorogenic response of **1** and **12** in HeLa cells. The cells were separately pretreated with media containing PX-12 (0, 2, and 10 μM) for 24 h at 37 °C. The media were replaced with PBS containing **1** (5.0 μM) and **12** (1.0 μM), respectively. After incubation for 10 min at 37 °C, the fluorescence images were recorded. The histogram is based on the averaged fluorescence intensity (FI) of each cell in the displayed images and shows the standard deviation as error bars (n = 5). (b) Effect of removing Trx by immunoprecipitation (IP) on the fluorescence of **1** (10.0 μM): before (crude) and after (IP supernatant). Time course of the fluorescence change of **1** in the protein extract (1.0 mg/mL). (c) Fluorescence enhancement of **1** in crude and IP-S. The excitation and emission wavelengths were 485 and 535 nm, respectively. The immunoreactivity of crude and IP-S are shown in a Western blot.

cells treated with **1** decreases in a PX-12 dose-dependent manner. In contrast, the fluorescence from **12** is unchanged under similar experimental conditions (lower panels in Figure 3). The removal of Trx from the crude extract of HeLa cells by immunoprecipitation (IP) also significantly reduced the FI ascribed to probe **1** and its environmental response (Figure 3b,c).

dx.doi.org/10.1021/ja503356q | J. Am. Chem. Soc. 2014, 136, 8430–8437

As further controls, studies were carried out in the presence of bacitracin, an inhibitor of protein disulfide isomerase (PDI),[24] and in the presence of E64, an inhibitor of other Cys-containing proteins.[25] In the case of both test experiments, little in the way of fluorescent changes were observed for probe **1** (Figure S11). Together with the data presented in Figure 3, we thus conclude that the disulfide bond cleavage reaction of **1** is predominantly caused by Trx in cells, and not by PDI, Cys-containing proteins, or other cytosolic protein thiols. To the extent this conclusion is correct, it leads to the suggestion that probe **1** can be used to test for the presence of absence of Trx at or near cell membranes, as well as its secretion from those loci into the extracellular space in response to an inflammatory insult.[13] This hypothesis was further tested via a series of experiments as detailed below.

A first set of studies involved testing a possible mode of Trx action. Recently, it was suggested that the anti-inflammatory effect of Trx involves a complex between Trx and TXNIP (thioredoxin-interacting protein).[26,27] According to this suggestion, under conditions of oxidative stress, Trx is oxidized and the TXNIP is released to bind to NLRP3 in an inflammasome; this activates its inflammatory response, including IL-1β secretion.[28] To investigate whether the proposed Trx activity shown in Figures 2 and 3 involves the Trx-TXNIP complex, the fluorogenic reaction of **1** was monitored in the presence of okadaic acid (OKA). OKA is an inhibitor of phosphoprotein phosphatases.[29] It reduces the concentration of TXNIP, which in turn increases the activity of Trx.[30,31] In the present study, HepG2 cells were separately pretreated with OKA (0, 50, and 100 nM, respectively). The media were then replaced with fresh media containing 5.0 μM of probe **1**, and the images were monitored as a function of time (recorded at 1, 5, 20, and 60 min after addition). As can be seen from an inspection of Figure 4, the fluorogenic response of **1** gradually increases as

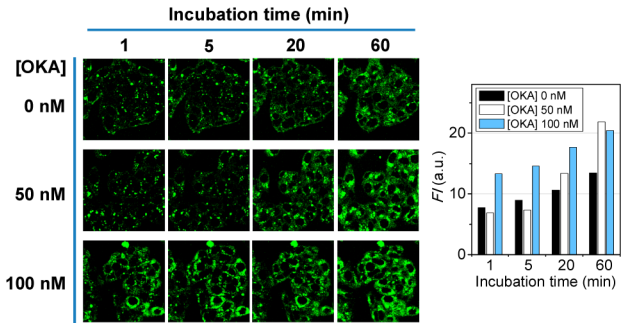

Figure 4. Fluorescence change of **1** in HepG2 cells treated with okadaic acid (OKA). Cells were separately pretreated with media containing OKA (0, 50, and 100 nM, respectively) for 1 h at 37 °C. The media were replaced with PBS containing **1** (5.0 μM). The images were then obtained at time points consisting of 1, 5, 20, and 60 min post addition at 37 °C. The histogram shows the averaged fluorescence intensity (FI) of each cell in the displayed images.

the concentration of OKA increases. This leads us to suggest that the increased fluorogenic response produced by **1** reflects the increase in Trx activity produced upon OKA inhibition of TXNIP.

To confirm the presence of a Trx-TXNIP complex in HepG2 cells, colocalization experiments with Trx, TXNIP, and NLRP3 were carried out using immunofluorescence analysis. Figure S12 displays the confocal immunofluorescence images, their overlay images, and the corresponding Z-stack orthogonal images (3D image). The image produced by Trx mainly overlaps with that of TXNIP (panels a–e), but not with that of NLRP3 (panels f–j). Also, as can be seen from an inspection of panels e and j in Figure S12, the Z-stack orthogonal images are consistent with the suggestion that the Trx overlaps with TXNIP in a focal plane. In contrast, no overlap is seen with NLRP3. The results provide further support for the previously stated conclusion, namely that Trx forms a complex with TXNIP and, as a result, these two species colocalize within the cell.

Having established that the fluorogenic response of **1** is associated with Trx activity, we sought to determine whether it could be used to signal the loss of membrane-associated Trx upon secretion into the extracellular media in analogy to IL-1β secretion under conditions of inflammatory stimulation. The secretion of Trx can be increased by adding cycloheximide and dinitrophenol.[13] Therefore, the fluorescence response of **1** in HeLa cells, which has Trx on the cell membrane, was monitored in the presence of cycloheximide and dinitrophenol. The results are summarized in Figure 5. As can be seen from an

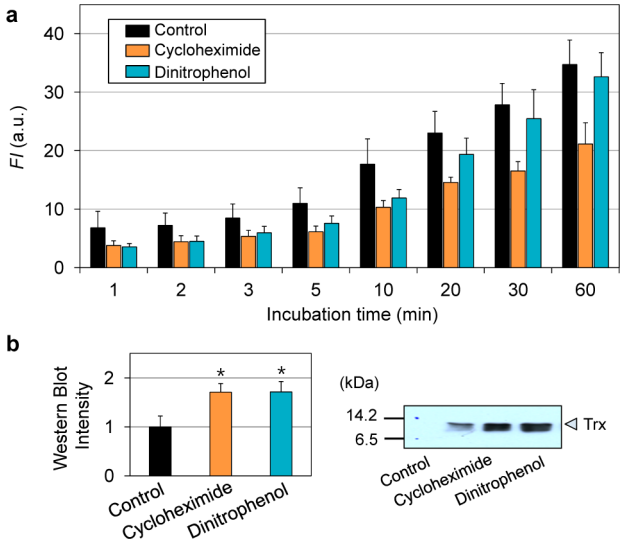

Figure 5. (a) Fluorescence change of **1** (5.0 μM) observed in HeLa cells treated with the Trx secretion activators cycloheximide (0.1 mM) and dinitrophenol (0.5 mM) for 3 h at 37 °C. Bars represent the averaged fluorescence intensity (FI) of each cell in confocal images recorded 1, 2, 3, 5, 10, 20, 30, and 60 min post treatment. (b) Western blot shows bands corresponding to the Trx (12 kDa) of cell culture medium in the absence and presence of cycloheximide or dinitrophenol. The histograms are based on the average and show the standard deviation as error bars (n = 4). Statistical significance is marked with a * when p < 0.05.

inspection of this figure, a reduced fluorescence response relative to untreated cells is seen after treatment with cycloheximide or dinitrophenol over the 1–60 min time range. This result is consistent with loss of membrane-localized Trx due to secretion over this time period (cf. Figures 5a and S13). As the incubation time increases, however, restoration of fluorescence is observed; presumably, this reflects regeneration of membrane-localized Trx and its reaction with unreacted probe **1**.

Confirmation that Trx is in fact secreted into the extracellular medium came from Western blot analyses of the cell culture media (Figure 5b). As expected, enhanced secretion of Trx was observed from the cells treated with cycloheximide or dinitrophenol. This provides further support for the conclusion

dx.doi.org/10.1021/ja503356q | J. Am. Chem. Soc. 2014, 136, 8430–8437

that probe **1** and its fluorogenic response may be used to monitor the induced secretion of Trx *in vitro*. Consistent with this supposition is the finding that compound **12** undergoes little change in its fluorescence character in cellular media containing cycloheximide or dinitrophenol (Figure S14). Similar experiments were also performed with the mitochondrial Trx-responding probe that we previously reported.[18] Here again, and in marked contrast to what was seen for **1**, little fluorescence change was observed under conditions favoring the secretion of Trx (Figure S15).

To test whether probe **1** might have utility as a potential diagnostic of inflammation, a hepatotoxic cellular model for fatty liver disease was used.[32] In these tests, HepG2 cells were treated with palmitic acid (PA) and oleic acid (OA). An excess of PA is known to induce oxidative stress,[33] endoplasmic reticulum stress,[34] mitochondrial malfunction,[35] and inflammation[36] in HepG2 cells. The underlying cytotoxic process is considered to be similar to hepatosteatosis, a condition known as fatty liver disease.[37] In contrast, OA is less cytotoxic toward HepG2 cells.[38] As seen in confocal images and the corresponding histograms of Figure 6a, PA-treated cells containing **1** produce a diminished fluorescence response near the cell membrane, while OA-treated cells are characterized by a fluorescence that matches that of cells containing only the probe. Moreover, an increase in the anti-Trx immunoreactivity was observed in the case of PA treatment relative to what was seen for the untreated group or cells exposed to OA (Figure 6b). Confocal imaging (cf. Figure 6c) provided further support for the notion that the anti-Trx immunoreactivity was decreased in the case of the PA-treated cells as compared to the untreated or the OA-treated cells (see also Figure S16).

Finally, the fluorogenic activity of **1** was checked in the HT-29 cell line (Figure S17). Again, a Trx-induced fluorescence increase was found around the cell membrane. Based on these findings, we conclude that **1** could have a role to play as a probe that is used to screen drug candidates, including potential anti-inflammatory agents, which mediate the effects of Trx secretion. The contribution to the fluorogenic reaction of probe **1** by the secreted Trx in plasma and serum would be anticipated to be negligible since in these loci [Trx] is in the nanomolar range[39] and in a relatively more-oxidized redox state than intracellular Trx.[40] Thus, we suggest that probe **1** and other rationally designed, site-selective Trx probes could be useful to play in differentiating between various diseases associated with oxidative stress without the need for invasive procedures such as tissue biopsies.

CONCLUSIONS

Reported here is a potential chemical marker for inflammatory disease, probe **1**. This membrane-targeting system produces a highly selective fluorescent response in the presence of Trx but not other biological thiols or other potential interferants. Confocal microscopic studies with the HepG2 cell line provide support for the design expectation that **1** interacts preferentially with the lipophilic cell membrane and produces a strong fluorescence response in the presence of membrane-associated Trx. This fluorogenic response may be regulated via formation of a Trx-TXNIP complex at or near the cell membrane. The effects of dinitrophenol and cycloheximide, which serve to enhance Trx secretion into the extracellular medium, could be readily monitored using **1** as a probe in studies involving HeLa cells. The potential utility of **1** as an indicator of pathogenic states and as a possible screening tool for agents that can manipulate secretion of membrane-associated Trx was demonstrated using a fatty liver disease model in HepG2 cells. Preliminary studies confirmed that **1** is also active as a Trx probe in the HT-29 cell line. On the basis of these findings, we suggest that this system could have a role to play in the screening of new potential anti-inflammatory drugs and in the

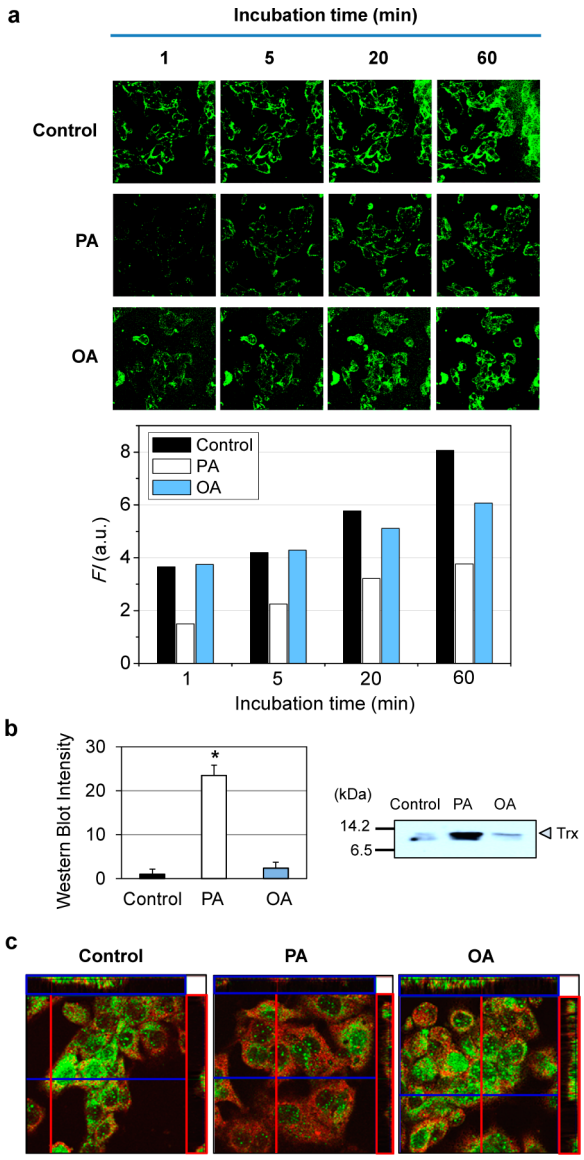

Figure 6. (a) Fluorescence change of **1** observed in HepG2 cells treated with fatty acids as a model of hepatosteatosis. Cells were separately pretreated with 0.7 mM of palmitic acid (PA) and oleic acid (OA) for 24 h at 37 °C. Fluorescence images of **1** were recorded at the following time points: 1, 5, 20, 60 min. The histogram shows the averaged fluorescence intensity (FI) of each cell in the images. (b) Western blot shows bands corresponding to the Trx (12 kDa) of cell culture medium in the absence and presence of PA or OA. The histograms are based on the average and show the standard deviation as error bars ($n = 4$). Statistical significance was marked with a * when $p < 0.05$. (c) Confocal immunofluorescence images of the fixed HepG2 cells (untreated, PA-treated, OA-treated cells) with antibodies for Trx (green) and NLRP3 (red). Fluorescence Z-stack orthogonal images were collected at 1 μm intervals ranging from 0 to 9 μm along a Z-optical axis.

dx.doi.org/10.1021/ja503356q | J. Am. Chem. Soc. 2014, 136, 8430−8437

diagnosis and staging of inflammation-related disease via optical methods that obviate the need for invasive procedures.

EXPERIMENTAL SECTION

Synthetic and Spectroscopic Methods. A complete listing of the methods used to prepare and characterize all new compounds, including probe 1, is included in the Supporting Information.

Liposome Preparation. Liposomes were prepared by the solvent evaporation method.[20] Briefly, 36 μL of (1,2-dipalmitoyl-*sn*-glycero-3-phosphocholine) DPPC (0.1 M in chloroform) and 24 μL of cholesterol (0.1 M in chloroform) were added to a 50 mL round-bottom flask containing 940 μL of chloroform and 200 μL of methanol. The aqueous phase (7 mL of HEPES buffer, 10 mM, pH 7.4) was then carefully added along the flask walls. The organic solvents were removed in a rotary evaporator under reduced pressure at 40 °C and 40 rpm. Subsequently, the resulting aqueous solution was subjected to sonication for 30 min. The liposomes were characterized by TEM (Figure S4). To stain the liposomes, a small amount of **1** in DMSO was added with measurements being made after 1 h at 37 °C. The [**1**]:[liposome] ratio was around 1:170.

Cell Culture and Imaging. A human cervical cancer cell line (HeLa) and a human hepatoma cell line (HepG2) were cultured in Dulbecco's Modified Eagle's Medium (DMEM) and in RPMI 1640, respectively, each supplemented with 10% FBS (WelGene), penicillin (100 units/mL), and streptomycin (100 μg/mL). Two days before imaging, the cells were placed on glass-bottomed dishes (MatTek) which were incubated in a humidified atmosphere containing 5% (v/v) CO_2 at 37 °C. Cell images were obtained using confocal microscopes from Leica (Leica model TCS SP2) and Zeiss (Zeiss model LSM 510). All fluorescence images of probe **1** were obtained using an excitation wavelength of 458 nm and a long path (>505 nm) emission filter. Other information is available in the Figure captions.

Treatment of HeLa Cells with Cycloheximide and Dinitrophenol. For the tests of Trx secretion from HeLa cells, the cells were plated at the 2×10^5/well level in glass-bottom dishes. After incubation overnight, the cells were treated with DMEM containing 0.5 mM dinitrophenol or 0.1 mM cycloheximide for 3 h at 37 °C. The media were exchanged for PBS containing **1** (5.0 μM) prior to confocal microscopic imaging.

Treatment of HpG2 Cells with Fatty Acids. HepG2 cells were plated at 2×10^5/well in glass-bottom dishes and incubated for 24 h. The media were changed to one containing 0.7 mM OA or 0.7 mM PA with bovine serum albumin (BSA) for 24 h at 37 °C. The media were then replaced with RPMI (Roswell Park Memorial Institute) medium without FBS for 4 h. Finally, the cells were incubated with PBS containing **1** (5.0 μM) prior to confocal microscopic imaging.

Western Blot Experiments. To collect Trx protein that was presumably secreted into the extracellular medium, media from each well were treated with 20% trichloroacetic acid for 30 min in ice and centrifuged at 14 000 rpm for 15 min at 4 °C. The resulting pellet was washed with 200 μL cold acetone and centrifuged two more times before being dried for 10 min by exposure to the laboratory atmosphere to remove the acetone. After being air-dried in this way, the pellet was resuspended in a sodium dodecyl sulfate–polyacrylamide gel electrophoresis (SDS-PAGE) sample buffer. The secreted Trx was separated by SDS-PAGE (15% polyacrylamide) and blotted onto a PVDR membrane (pore size 0.2 μm) using a Bio-Rad Transblot kit (Trans-Blot SD semi-dry transfer cell kit, Bio-Rad, Inc., CA). The membrane was treated with a blocking solution (5% (w/v) nonfat dry milk in TBS-T) for 1 h at room temperature, before being subjected to primary antibody binding using goat anti-Trx antibody (ab16965, Abcam, Inc., MA); this was done using a blocking solution and overnight treatment at 4 °C. The excess antibody was removed by rinsing three times with TBS-T. For the secondary antibody binding studies, the membrane was incubated with a donkey anti-goat IgG-HRP antibody (sc-2005, Santa Cruz, Inc., Texas) in a blocking solution for 1 h at room temperature. After the membrane was rinsed with TBS-T buffer 3 times, the immunoreactive bands were detected via treatment with an ECL substrate solution (Western Blot Detection System, iNtRON, Inc., Kyunggi-do, Korea), followed by visualization on X-ray film (AGFA). The density ratio was normalized to that of the control. The values are expressed as mean ± SD, with an $n = 4$ (i.e., four independent samples from different cells). Data were analyzed statistically by the Student's t test, and a value of $p < 0.05$ was considered to be statistically significant.

Immunohistochemistry-Based Colocalization of Trx with TXNIP or NLRP3. Cells in PBS solution were fixed with 4% paraformaldehyde in PBS for 30 min at room temperature and washed with a buffer (0.1% BSA and 0.1% Triton X-100). The fixed cells were blocked with a blocking buffer (1% BSA). After the blocking buffer was discarded, the cells were incubated with rabbit anti-Trx antibody (1:200, diluted with 0.1% BSA) overnight at 4 °C. After removal of the unbound antibody, the cells were incubated with goat anti-TXNIP or mouse anti-NLRP3 antibodies (1:200, diluted with 0.1% BSA) for 1 h at room temperature, followed by washing with the above buffer 3 times. The cells were incubated with the corresponding fluorescent secondary antibodies (1:1000, diluted with 0.1% BSA) for 1 h at room temperature. Finally, after washing, the fluorescence images of the cells were obtained based on a Z-stack (3D image stack) using a confocal microscope (Zeiss LSM 510 model) where the Z-stack images were collected at 1 μm intervals over a 0–9 μm range. Merged Z-stack and orthogonal images were then obtained. Trx (ab26320, Abcam, Inc., MA), TXNIP (SC-33099, Santa Cruz, Inc., TX), and NLRP3 (Cryo-2, Adipogen, Inc., Incheon, Korea) were detected using 488 donkey anti-rabbit IgG, 546 rabbit anti-goat IgG, and 633 goat anti-mouse IgG (A-21206, A-21085, and A-21050 from Molecular Probes, Inc., OR) antibodies. The images corresponding to Trx (green), TXNIP (red), and NLRP3 (red) were obtained using excitation wavelengths of 488, 543, and 633 nm and 505–530 nm band-path, 560 nm long-path, and 650 nm long-path filters, respectively.

ASSOCIATED CONTENT

Supporting Information

Synthetic and spectroscopic methods, additional spectra (UV/vis absorption, fluorescence, NMR, ESI-MS, and MALDI-TOF MS), and imaging data. This material is available free of charge via the Internet at http://pubs.acs.org.

AUTHOR INFORMATION

Corresponding Authors

kangch@khu.ac.kr
sessler@cm.utexas.edu
jongskim@korea.ac.kr

Notes

The authors declare no competing financial interest.

ACKNOWLEDGMENTS

This work was supported by National Research Foundation of The Ministry of Science, ICT & Future Planning in Korea (No. 2009-0081566, J.S.K.; NRF-2012R1A6A3A03037981, M.H.L.), Cooperative Research Program for Agriculture Science & Technology Development (No. PJ008959, C.K.), the U.S. National Institutes of Health (CA 68687, J.L.S.), and the Robert A. Welch Foundation (F-1018, J.L.S.).

REFERENCES

(1) (a) Holmgren, A.; Bjornstedt, M. *Methods Enzymol.* **1995**, *252*, 199–208. (b) Nakamura, H.; Nakamura, K.; Yodoi, J. *Annu. Rev. Immunol.* **1997**, *15*, 351–369.

(2) Mustacich, D.; Powis, G. *Biochem. J.* **2000**, *346*, 1–8.

(3) (a) Arnér, E. S. J.; Holmgren, A. *Eur. J. Biochem.* **2000**, *267*, 6102–6109. (b) Bindolia, A.; Rigobello, M. P.; Scutari, G.; Gabbiani, C.; Casini, A.; Messori, L. *Coord. Chem. Rev.* **2009**, *253*, 1692–1707. (c) Holmgren, A.; Johansson, C.; Berndt, C.; Loenn, M. E.; Hudemann, C.; Lillig, C. H. *Biochem. Soc. Trans.* **2005**, *33*, 1375–1377.

(4) (a) Watson, W. H.; Pohl, J.; Montfort, W. R.; Stuchlik, O.; Reed, M. S.; Powis, G.; Jones, D. P. *J. Biol. Chem.* **2003**, *278*, 33408−33415. (b) Pekkari, K.; Holmgren, A. *Antiox. Redox Signal.* **2004**, *6*, 53−61.
(5) Gasdaska, J. R.; Berggren, M.; Powis, G. *Cell Growth Differ.* **1995**, *6*, 1643−1650.
(6) Haendeler, J.; Hoffman, J.; Tischler, V.; Berk, B. C.; Zeiher, A. M.; Dimmeler, S. *Nat. Cell Biol.* **2002**, *4*, 743−749.
(7) (a) Bertini, R.; Howard, O. M.; Dong, H. F.; Oppenheim, J. J.; Bizzarri, C.; Sergi, R.; Caselli, G.; Pagliei, S.; Romines, B.; Wilshire, J. A.; Mengozzi, M.; Nakamura, H.; Yodoi, J.; Pekkari, K.; Gurunath, R.; Holmgren, A.; Herzenberg, L. A.; Ghezzi, P. *J. Exp. Med.* **1999**, *189*, 1783−1789. (b) Lu, Y.; Zhao, X.; Li, K.; Luo, G.; Nie, Y.; Shi, Y.; Zhou, Y.; Ren, G.; Feng, B.; Liu, Z.; Pan, Y.; Li, T.; Guo, X.; Wu, K.; Miranda-Vizuete, A.; Wang, X.; Fan, D. *Antiox. Redox Signal.* **2013**, *19*, 899−911. (c) Tiitto, L.; Kaarteenaho-Wiik, R.; Sormunen, R.; Holmgren, A.; Paakko, P.; Soini, Y.; Kinnula, V. *J. Pathol.* **2003**, *201*, 363−370.
(8) Csiki, I.; Yanagisawa, K.; Haruki, N.; Nadaf, S.; Morrow, J. D.; Johnson, D. H.; Carbone, D. P. *Cancer Res.* **2006**, *66*, 143−150.
(9) Shioji, K.; Nakamura, H.; Masutani, H.; Yodoi, J. *Antiox. Redox Signal.* **2003**, *5*, 795−802.
(10) Advani, A.; Gilbert, R. E.; Thai, K.; Gow, R. M.; Langham, R. G.; Cox, A. J.; Connelly, K. A.; Zhang, Y.; Herzenberg, A. M.; Christensen, P. K.; Pollock, C. A.; Qi, W.; Tan, S. M.; Parving, H.-H.; Kelly, D. J. *J. Am. Soc. Nephrol.* **2009**, *20*, 730−741.
(11) Matsuo, Y.; Yodoi, J. *Cytokine Growth Factor Rev.* **2013**, *24*, 345−353.
(12) (a) Shan, W.; Zhong, W.; Zhao, R.; Oberley, T. D. *Free Radic. Biol. Med.* **2010**, *49*, 2078−2087. (b) Nagano, M.; Hatakeyama, K.; Kai, M.; Nakamura, H.; Yodoi, J.; Asada, Y.; Chijiiwa, K. *HPB (Oxford)* **2012**, *14*, 573−582. (c) Soini, Y.; Kahlos, K.; Napankangas, U.; Kaarteenaho-Wiik, R.; Saily, M.; Koistinen, P.; Paakko, P.; Holmgren, A.; Kinnula, V. L. *Clin. Cancer Res.* **2001**, *7*, 1750−1757.
(13) Rubartelli, A.; Bajetto, A.; Allavena, G.; Wollman, E.; Sitia, R. *J. Biol. Chem.* **1992**, *267*, 24161−24164.
(14) Söderberg, A.; Sahaf, B.; Rosén, A. *Cancer Res.* **2000**, *60*, 2281−2289.
(15) Sahaf, B.; Soderberg, A.; Spyrou, G.; Barral, A. M.; Pekkari, K.; Holmgren, A.; Rosen, A. *Exp. Cell Res.* **1997**, *236*, 181−192.
(16) Wollman, E. E.; Kahan, A.; Fradelizi, D. *Biochem. Biophys. Res. Commun.* **1997**, *230*, 602−606.
(17) (a) Schenk, H.; Vogt, M.; Dröge, W.; Schulze-Osthoff, K. *J. Immunol.* **1996**, *156*, 765−771. (b) Rosen, A.; Lundman, P.; Carisson, M.; Bhavani, K.; Srinivasa, B. R.; Kjellström, G.; Nilsson, K.; Holmgren, A. *Int. Immunol.* **1995**, *7*, 625−633. (c) Blum, H.; Rollinghoff, M.; Gessner, A. *Cytokine* **1996**, *8*, 6−13. (d) Matsuda, M.; Masutani, H.; Nakamura, H.; S, M.; Yamauchi, A.; Yonehara, S.; Uchida, A.; K, I.; Horiuchi, A.; Yodoi, J. *J. Immunol.* **1991**, *147*, 3837−3841.
(18) Lee, M. H.; Han, J. H.; Lee, J.-H.; Choi, H. G.; Kang, C.; Kim, J. S. *J. Am. Chem. Soc.* **2012**, *134*, 17314−17319.
(19) Bhat, G. B.; Iwase, L.; Hummel, B. C. W.; Walfish, P. G. *Biochem. J.* **1989**, *258*, 785−792.
(20) Moscho, A.; Orwar, O.; Chiu, D. T.; Modi, B. P.; Zare, R. N. *Proc. Natl. Acad. Sci. U.S.A.* **1996**, *93*, 11443−11447.
(21) Rodal, S. K.; Skretting, G.; Garred, O.; Vilhardt, F.; van Deurs, B.; Sandvig, K. *Mol. Biol. Cell* **1999**, *10*, 961−974.
(22) Hommelgaard, A. M.; Roepstorff, K.; Vilhardt, F.; Torgersen, M. L.; Sandvig, K.; van Deurs, B. *Traffic* **2005**, *6*, 720−724.
(23) Kirkpatrick, D. L.; Kuperus, M.; Dowdeswell, M.; Potier, N.; Donald, L. J.; Kunkel, M.; Berggren, M.; Angulo, M.; Powis, G. *Biochem. Pharmacol.* **1998**, *55*, 987−994.
(24) Mandel, R.; Ryser, H. J.; Ghani, F.; Wu, M.; Peak, D. *Proc. Natl. Acad. Sci. U.S.A.* **1993**, *90*, 4112−4116.
(25) Huber, K.; Patel, P.; Zhang, L.; Evans, H.; Westwell, A. D.; Fischer, P. M.; Chan, S.; Martin, S. *Mol. Cancer Ther.* **2008**, *7*, 143−151.
(26) Nishiyama, A.; Matsui, M.; Iwata, S.; Hirota, K.; Masutani, H.; Nakamura, H.; Takagi, Y.; Sono, H.; Gon, Y.; Yodoi, J. *J. Biol. Chem.* **1999**, *274*, 21645−21650.
(27) World, C.; Spindel, O. N.; Berk, B. C. *Arterioscler. Thromb. Vasc. Biol.* **2011**, *31*, 1890−1897.
(28) Zhou, R.; Tardivel, A.; Thorens, B.; Choi, I.; Tschopp, J. *Nat. Immunol.* **2010**, *11*, 136−140.
(29) Robinson, K. A.; Brock, J. W.; Buse, M. G. *J. Mol. Endocrinol.* **2013**, *50*, 59−71.
(30) Turturro, F.; Friday, E.; Welbourne, T. *BMC Cancer* **2007**, *7*, 96−102.
(31) Yamawaki, H.; Pan, S.; Lee, R. T.; Berk, B. C. *J. Clin. Invest.* **2005**, *115*, 733−738.
(32) Li, Z. Z.; Berk, M.; McIntyre, T. M.; Gores, G. J.; Feldstein, A. E. *Hepatology* **2008**, *47*, 1495−1503.
(33) Srivastava, S.; Chan, C. *Free Radic. Res.* **2007**, *41*, 38−49.
(34) Achard, C. S.; Laybutt, D. R. *Endocrinology* **2012**, *153*, 2164−2177.
(35) Ji, J.; Zhang, L.; Wang, P.; Mu, Y.-M.; Zhu, X.-Y.; Wu, Y.-Y.; Yu, H.; Zhang, B.; Chen, S.-M.; Sun, X.-Z. *Exp. Toxicol. Pathol.* **2005**, *56*, 369−376.
(36) Joshi-Barve, S.; Barve, S. S.; Amancherla, K.; Gobejishvili, L.; Hill, D.; Cave, M.; Hote, P.; McClain, C. J. *Hepatology* **2007**, *46*, 823−830.
(37) Tuyama, A. C.; Chang, C. Y. *J. Diabetes* **2012**, *4*, 266−280.
(38) Maedler, K.; Oberholzer, J.; Bucher, P.; Spinas, G. A.; Donath, M. Y. *Diabetes* **2003**, *52*, 726−733.
(39) Mongardon, N.; Lemiale, V.; Borderie, D.; Burke-Gaffney, A.; Perbet, S.; Marin, N.; Charpentier, J.; Pène, F.; Chiche, J.-D.; Mira, J.-P.; Cariou, A. *Critical Care* **2013**, *17*, R18.
(40) Chaiswing, L.; Oberley, T. D. *Antiox. Redox Signal.* **2010**, *13*, 449−465.